MORPHOLOGICAL CONTROL OF LAYERED M_OS_2 VIA TWO-ZONE CHEMICAL VAPOR DEPOSITION: A STUDY ON GROWTH PARAMETERS

Akanksha AGARWAL[1,2], Dhananjay K. SHARMA[2], Kateřina Aubrechtová DRAGOUNOVÁ[2], Rajarshi ROY[2], Štěpán POTOCKÝ[1,2], Alexander KROMKA[2]

[1]*Faculty of Electrical Engineering, Czech Technical University, Technická 1902/2, 166 27 Praha 6, Czech Republic, EU, agarwaka@fel.cvut.cz*

[2]*Institute of Physics of the Czech Academy of Sciences, Cukrovarnická 10/112, 162 00, Prague 6, Czech Republic, EU, akanksha@fzu.cz*

https://doi.org/10.37904/nanocon.2025.5182

Abstract

Two-dimensional (2D) molybdenum disulfide (MoS_2) synthesized by Chemical Vapor Deposition (CVD) is essential for scalable electronic and optoelectronic applications. We report a systematic study on the CVD synthesis of MoS_2 layers on Si/SiO_2 substrates using MoO_3 and sulfur powder precursors in a two-zone furnace. This work investigates the influence of key parameters in CVD growth, including substrate orientation (horizontal and vertical), growth temperature, carrier gas flow rate, and pressure on the resulting growth, nucleation density, and flake morphology. Our characterization relies primarily on optical microscopy to analyze nucleation density, crystal domain size, and flake geometry. We demonstrate that slight variations dictate the transition from high-density, small-domain films to low-density, large-area single crystals, directly correlating synthesis conditions to the quality of the resulting 2D material. With the chosen parameter window, we obtain well-defined triangular domains consistent with a large area. We performed the Raman and photoluminescence (PL) spectroscopy measurements to confirm the growth of MoS_2 layers. These morphological observations provide crucial insights into the underlying growth kinetics and offer a roadmap for the controlled synthesis of large areas. Our findings contribute to the optimization of scalable synthesis routes for high-quality MoS_2 films for electronic and optoelectronic applications.

Keywords: Chemical vapor deposition, MoS_2, optical microscopy, Raman spectroscopy, photoluminescence

1. INTRODUCTION

Transition metal dichalcogenides have attracted significant attention due to their layer-dependent bandgap, high carrier mobility, and potential applications in nanoelectronics, photodetectors, and energy-harvesting devices [1, 2]. 2D MoS_2 has emerged as a promising material due to its tunable bandgap and excellent electronic properties, making it suitable for optoelectronic applications [3, 4]. Monolayer MoS_2 exhibits a direct bandgap (~1.8 eV) [5]. CVD enables the scalable growth of large-area MoS_2 films with controlled thickness, which is a critical factor for practical applications [6]. Despite extensive research, reproducible control of nucleation density and lateral domain size, as well as achieving uniform monolayer growth with minimal intermediate phases (e.g., MoO_{3-x} or a mixed-phase intermediate compound such as $MoOS_2$), remains challenging [7]. The CVD process typically involves sulfurization of MoO_3 in a two-zone furnace. This manuscript examines the CVD synthesis process, focusing on the chemical reactions involved and the influence of experimental parameters, including precursor and substrate temperatures, carrier gas flows, and deposition times. Optical microscopy, a cost-effective and non-destructive tool, is used to assess film quality, providing insights into domain structure and layer uniformity. Optimized conditions yield uniform MoS_2 layers with distinct optical contrast, indicating few-layer structures. Our results provide essential feedback for tuning the CVD process to optimize the crystalline morphology for future device fabrication.

2. EXPERIMENTAL METHODS

2.1. MoS_2 Synthesis via CVD

MoS_2 films were synthesized on Si/SiO_2 (300 nm SiO_2 layer on bare Si) substrates using a dual-zone thermal CVD system [8]. Prior to the deposition, the substrates were cleaned using ultrasonication in acetone and isopropanol for 10 minutes each, followed by a 5 minute rinse in deionized water and finally, 10 minutes in an oxygen plasma. MoO_3 (Sigma-Aldrich, 99.97 %, 14 mg) and sulfur (Sigma-Aldrich, 99.00 %, 90 mg) powders were used as precursors and placed in separate boats within the CVD furnace (see **Figure 1b**). The cleaned substrates were positioned face down on the MoO_3 boat (as shown in the schematic diagram in **Figure 1**). The sulfur boat was placed in the lower temperature zone, while the MoO_3 boat was located downstream in the higher temperature zone. The distance between the MoO_3 and sulfur sources within the furnace was approximately 20 cm. The deposition process consisted of temperature ramps as shown in **Figure 1e**. Initially, the temperature of the MoO_3 zone (high-temperature zone) is set to 550 °C at a rate of 20 °C/minute, followed by a dwell time of 5 minutes. Subsequently, the MoO_3 zone temperature was further raised to the growth temperature (e.g., 850 °C) at a slower rate of 5 °C/minute, and at the same time, the sulfur zone temperature was raised from room temperature to 150 °C. After reaching the growth temperature, the deposition was carried out for 20 minutes and the sulfur zone temperature was kept constant at 150 °C during the deposition period. A constant nitrogen gas flow (e.g., 200 sccm (standard cubic centimeters per minute)) was maintained throughout the experiment under different pressures, such as vacuum (~10^{-2} mbar) or atmospheric pressure (measured value ~980 mbar). After deposition, the furnace cooled down naturally.

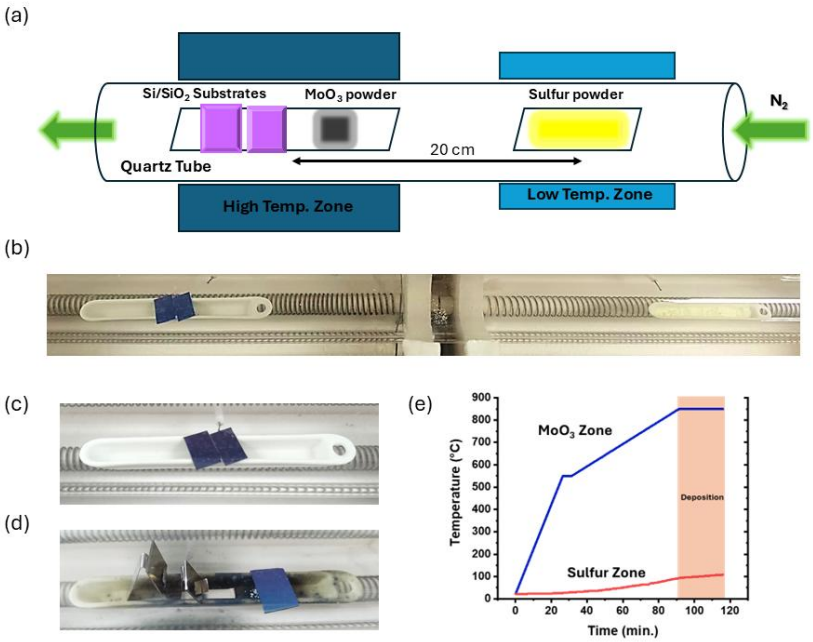

Figure 1 Visualization of CVD configuration and growth parameters: (a) schematic of two-zone CVD furnace, (b) arrangement of precursor (MoO_3 and sulfur) boats and Si/SiO_2 substrate within the quartz tube, (c) horizontal orientation of the substrate placement, (d) vertical orientation of the substrate placement, (e) temperature ramp for the MoO_3 (growth temperature 850 °C) and sulfur zone temperature profiles showing the heating ramps for the high-temperature (MoO_3 – blue line) and low-temperature (sulfur – red line) zones.

2.2. Parameter Modulation

A systematic study was performed by varying three primary parameters (flow rate, pressure, and growth temperature) while keeping other parameters constant.

Table 1 CVD parameters for the synthesis of layered MoS_2.

Series	Growth Temperature (°C)	Pressure (mbar)	Flow rate (sccm)
flow	850 °C	Atmospheric	10 sccm
	850 °C	Atmospheric	50 sccm
	850 °C	Atmospheric	100 sccm
	850 °C	Atmospheric	200 sccm
pressure	800 °C	Vacuum	100 sccm
	800 °C	50 mbar	100 sccm
	800 °C	100 mbar	100 sccm
	800 °C	Atmospheric	100 sccm
temperature no. 1	800 °C	50 mbar	50 sccm
	750 °C	50 mbar	50 sccm
	700 °C	100 mbar	50 sccm
temperature no. 2	800 °C	50 mbar	100 sccm
	750 °C	50 mbar	100 sccm
	700 °C	100 mbar	100 sccm

2.3. Characterization

All the synthesized MoS_2 films were analyzed using a standard bright-field optical microscope (Olympus) equipped with 10×, 20×, 50×, and 100× objective lenses to analyze surface morphology, domain size, and layer thickness based on color contrast.

The Raman and photoluminescence (PL) spectra were measured by a Horiba LabRAM HR Evolution system (HORIBA Scientific). The measurements were performed using a 532 nm excitation wavelength source (Nd: YAG), equipped with an air-cooled CCD camera. Laser and scattered light were focused through an Olympus objective with a 100× magnification and an NA of 0.9 with ~1 μm spot focus. A grating of 1800 lines/mm and of 600 lines/mm was used for Raman and PL measurements, respectively.

3. RESULTS AND DISCUSSION

The formation of MoS_2 proceeds through a two-step vapor-phase reaction [9],

$$MoO_3 + x/2\ S \rightarrow MoO_{3-x} + x/2\ SO_2$$

$$MoO_{3-x} + (7-x)/2\ S \rightarrow MoS_2 + (3-x)/2\ SO_2$$

When the reaction time is short, the sulfurization process is incomplete, leading to the formation of intermediate compounds. Therefore, the 20-minute deposition time was chosen to ensure complete sulfurization and to minimize the presence of intermediate compounds, based on this reaction mechanism. We deposited MoS_2 in both horizontal and vertical substrate orientations, as shown in **Figure 1c and 1d**. In horizontal orientation, the substrate is positioned directly in the main gas flow stream and closest to the MoO_3 precursor boat, resulting in a higher effective local concentration of Mo-containing species. This orientation promotes rapid, high-density nucleation and continuous film growth, often leading to polycrystalline and non-homogeneous domains (**Figure 2a-c**). Conversely, the vertical orientation does not have the direct precursor flux, lowering the effective precursor saturation at the surface. This vertical orientation favors the growth of a large area and more homogeneous MoS_2 domains (**Figure 2d-f)**.

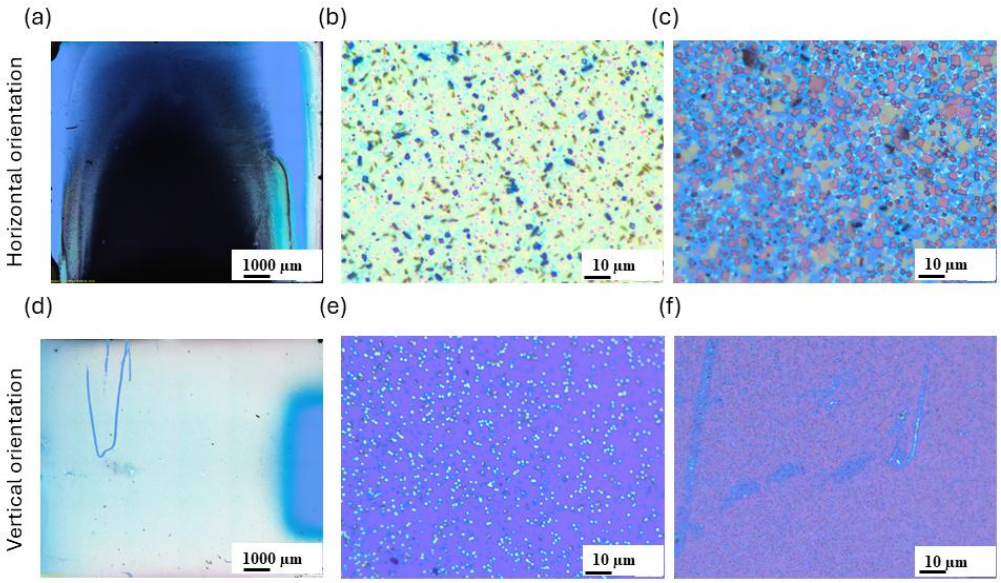

Figure 2 Impact of substrate orientation on MoS_2 film morphology: (a) and (d) complete sample overview (low-magnification views) of MoS_2 films grown on the horizontal and vertical substrate orientations, respectively; (b), (c) high-magnification images of the horizontally grown sample; (e), (f) high-magnification images of the vertically grown sample.

The flow rate of the carrier gas primarily affects the transport of the volatile Mo-precursor species and the gas flow above the substrate. **Figure 3** shows the optical images of the MoS_2 samples deposited at different flow rates at 850 °C, and all other parameters were kept constant. A N_2 flow of 50 and 100 sccm balanced the precursor transport and the homogeneity of the final deposit. Low flows (<50 sccm) limited the precursor delivery, i.e., sulfur atom delivery, while high flows (>200 sccm) disrupted the film continuity. As the carrier gas (N_2) flow rate decreases, the fluid velocity of sulfur atoms also decreases, allowing sufficient time for Mo atoms to react with S atoms. As a result, the as-formed MoS_2 grain grows larger, which is consistent with the experimental results. Therefore, there is a rapid change in the yield and density of MoS_2, indicating that the gas flow rate is a crucial parameter in the synthesis process, affecting both the nucleation and growth of MoS_2.

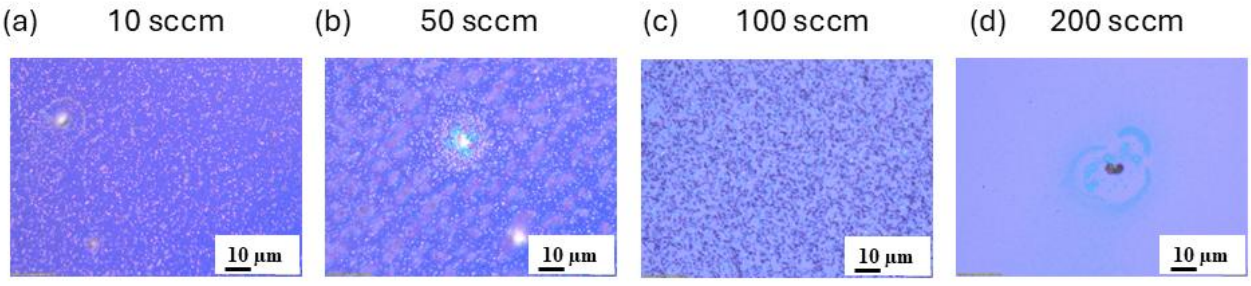

Figure 3 Optical microscopy images of the MoS_2 samples deposited at 850 °C at different N_2 flow rates (a) 10 sccm, (b) 50 sccm, (c) 100 sccm, and (d) 200 sccm.

The growth temperature in the MoO_3 zone is another critical parameter that governs the growth of MoS_2. Based on previous reports, the synthesis of MoS_2 typically requires a high reaction temperature [8]. However, our experimental results show successful synthesis even at a lower deposition temperature range (700-750 °C). A MoO_3 temperature of 700-800 °C ensured adequate vaporization. Lower temperatures led to incomplete reactions, while higher temperatures revealed irregular growth (**Figure 4**). The growth temperature has a

critical effect on nucleation density and layer thickness. Optimal large area monolayer growth was observed at ~750 °C and a flow rate of 50-100 sccm.

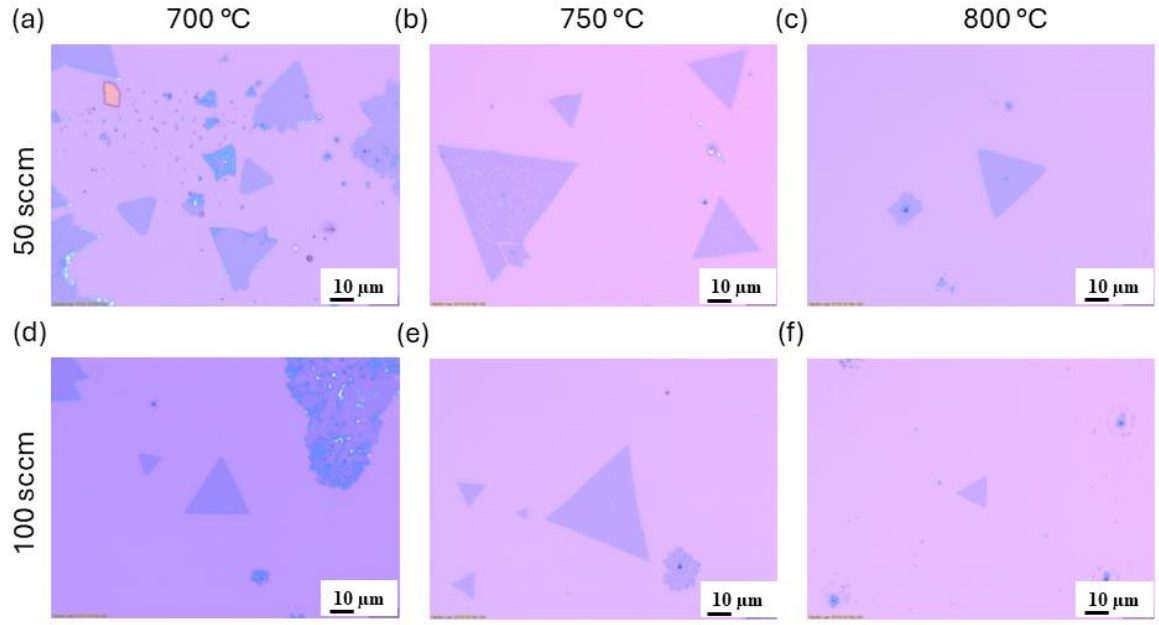

Figure 4 Optical microscopy images of the MoS_2 samples grown at different temperatures of 700 °C, 750 °C, 800 °C, and flow rates of 50 sccm and 100 sccm.

The pressure is another crucial parameter determining the stoichiometry and shape of the MoS_2 flakes. The optical images show a clear transition in flake morphology as pressure varied (**Figure 5**). First, atmospheric pressure resulted in uncontrolled nucleation and the formation of multilayer domains. Excess sulfur leads to high levels of gas-phase reactions and often results in residual sulfur deposits around the flakes, complicating the optical analysis and potentially increasing the number of stacked layers. Reduced pressure (50-100 mbar) improved uniformity and allowed the formation of triangular domains. Finally, very low pressure (vacuum) leads to insufficient precursor delivery, resulting in poor or no layer formation.

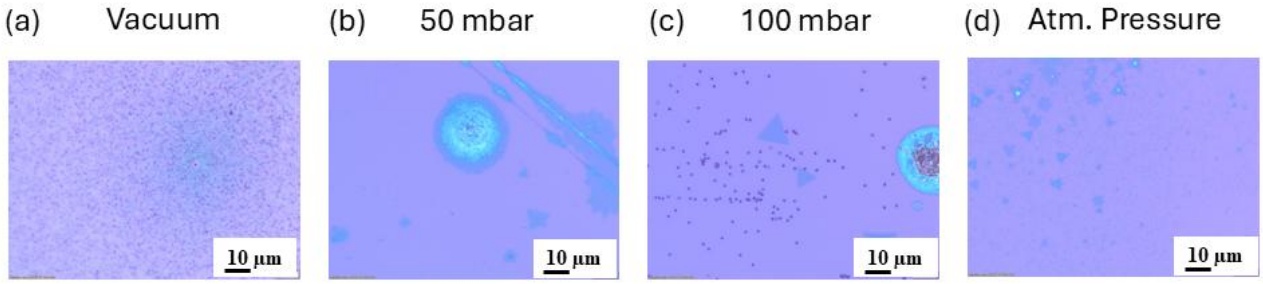

Figure 5 Optical microscopy images of MoS_2 samples deposited under different ambient pressures (a) vacuum, (b) 50 mbar, (c) 100 mbar, and (d) atmospheric pressure.

In **Figure 6a**, the Raman spectrum of an as-grown sample synthesized under optimal conditions (growth temperature 750 °C, pressure 50 mbar, and flow rate 50 sccm) confirms the successful growth of MoS_2. The spectrum contains two characteristic peaks located at positions around 382 and 403 cm^{-1}, corresponding to the E_{2g} mode representing the in-plane vibration and the A_{1g} mode related to the out-of-plane vibration of atoms [10], [11], respectively.

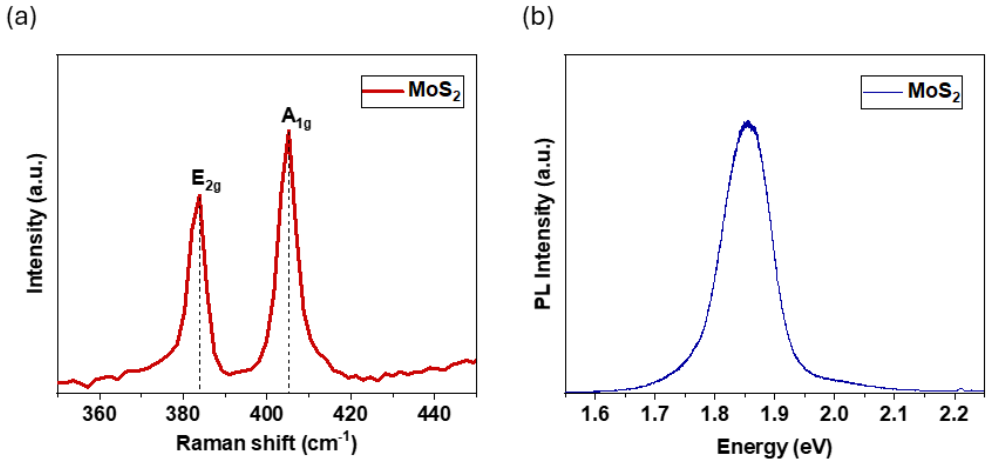

Figure 6 (a) Raman Spectra of MoS_2 (b) Photoluminescence spectra of MoS_2 of the sample grown at 750 °C, pressure 50 mbar, and flow rate 50 sccm.

Figure 6b shows the PL spectrum of the same MoS_2 sample, which exhibits a sharp luminescence peak at around 1.85 eV. This energy closely corresponds to the direct bandgap of monolayer MoS_2, highlighting its potential for optoelectronic applications.

We also performed polarization-dependent Raman spectroscopy to evaluate the crystalline quality and domain orientation. **Figure 7** shows the polar plot of the E_{2g} and A_{1g} Raman intensities as a function of the polarization angle. The observed periodic dependence, specifically the clear two-fold symmetry for both the E_{2g} and A_{1g} peaks, confirms the in-plane crystalline alignment of the MoS_2 flakes. This anisotropic behavior is indicative of high crystalline quality and a uniform domain orientation within the measured area. The combined results of optical microscopy (triangular domains), Raman peaks, and PL emission confirm that the samples grown under the optimized parameter window (growth temperature: 750 °C, pressure: 50 mbar, and flow rate: 50 sccm) are high-quality, crystalline, and suitable for further characterization. Our future work will focus on exploring the temperature-dependent effects on the Raman and PL spectra, which will provide deeper insights into the film's thermal stability and defect structure.

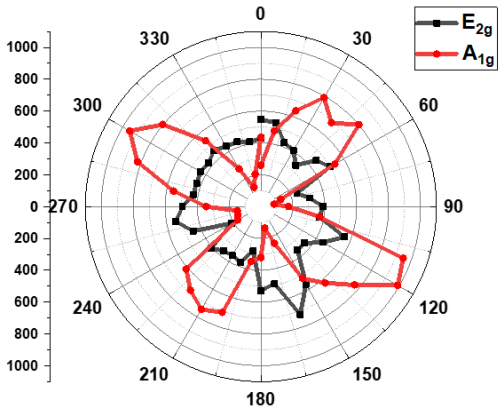

Figure 7 Polar plots of the E_{2g} and A_{1g} Raman intensities of MoS_2 as a function of the polarization angle.

4. CONCLUSION

We demonstrate that the reproducible synthesis of MoS_2 monolayers in a two-zone CVD furnace is enabled by precise control of temperature, pressure, and carrier gas flow rate. We have successfully correlated these

key parameters with the morphology of grown layered MoS_2 on Si/SiO_2 substrates, using optical microscopy. Optimal morphological control was achieved at a growth temperature of 750 °C, a pressure range of 50-100 mbar, and a flow rate range of 50-100 sccm. This growth window yields low-density, large-area, perfectly triangular MoS_2 domains, which are qualitatively indicative of high-quality, likely monolayer or few-layer films, as confirmed by the characteristic Raman peaks and direct bandgap PL emission (1.85 eV). Deviations from this window immediately resulted in high-density polycrystalline films, severe thickness non-uniformity (high optical contrast), or morphological imperfections.This work establishes a foundation for process tuning, demonstrating that the control of CVD growth kinetics can be effectively monitored and optimized solely through detailed morphological analysis, providing a rapid feedback loop for large-area growth optimization. These findings provide a pathway for the fabrication of 2D materials for device applications. Future work will involve confirming the layer number and crystalline quality of these optimized films using complementary techniques such as Raman spectroscopy and atomic force microscopy (AFM). Additionally, we plan to explore the temperature and magnetic-field-dependent effects on Raman and PL analysis to characterize the properties of the as-synthesized MoS_2 fully.

ACKNOWLEDGEMENTS

This work was supported by the MEYS OP JAC project SENDISO (no. CZ.02.01.01/00/22_008/0004596), used the infrastructure of the CzechNanoLab (no. LM2023051), and was partially supported by the CTU university project no. SGS24/131/OHK4/3T/13.

REFERENCES

[1] MANZELI, S., OVCHINNIKOV, D., PASQUIER, D., YAZYEV, O.V., KIS, A. 2D transition metal dichalcogenides. *Nature Reviews Materials*. 2017, vol. 2, pp. 17033.

[2] BUTLER, S.Z., et al. Progress, Challenges, and Opportunities in Two-Dimensional Materials Beyond Graphene. *ACS Nano*. 2013, vol. 7, pp. 2898–2926.

[3] MAK, K.F., LEE, C., HONE, J., SHAN, J., HEINZ, T.F. Atomically Thin MoS_2: A New Direct-Gap Semiconductor. *Phys. Rev. Lett.* 2010, vol. 105, pp. 136805.

[4] WANG, Q.H., KALANTAR-ZADEH, K., KIS, A., COLEMAN, J.N., STRANO, M.S. Electronics and optoelectronics of two-dimensional transition metal dichalcogenides. *Nature Nanotech*. 2012, vol. 7, pp. 699–712.

[5] SPLENDIANI, A., et al. Emerging Photoluminescence in Monolayer MoS_2. *Nano Letters*. 2010, vol. 10, pp. 1271–1275.

[6] LEE, Y., et al. Synthesis of Large-Area MoS_2 Atomic Layers with Chemical Vapor Deposition. *Advanced Materials*. 2012, vol. 24, pp. 2320–2325.

[7] MATHEW, S., et al. Three-Dimensional MoS_2 Nanosheet Structures: CVD Synthesis, Characterization, and Electrical Properties. *Crystals*. 2023, vol. 13, pp. 448.

[8] WANG, S., et al. Shape Evolution of Monolayer MoS_2 Crystals Grown by Chemical Vapor Deposition. *Chem. Mater.* 2014, vol. 26, pp. 6371–6379.

[9] LI, X.L., LI, Y.D. Formation of MoS_2 inorganic fullerenes (IFs) by the reaction of MoO_3 nanobelts and S. *Chemistry - A European Journal*. 2003, vol. 9, pp. 2726–2731.

[10] LI, H., et al. From bulk to monolayer MoS_2: Evolution of Raman scattering. *Advanced Functional Materials*. 2012, vol. 22, pp. 1385–1390.

[11] LEE, C., YAN, H., BRUS, L.E., HEINZ, T.F., HONE, J., RYU, S. Anomalous Lattice Vibrations of Single- and Few-Layer MoS_2. *ACS Nano*. 2010, vol. 4, pp. 2695–2700.